IEEE Photonics Journal
An IEEE Photonics Society Publication

Open Access

# Ultrabroadband Plasmonic Absorber Based on Biomimetic Compound Eye Structures

Volume 10, Number 1, February 2018

Xiaoxuan Dong
Linsen Chen

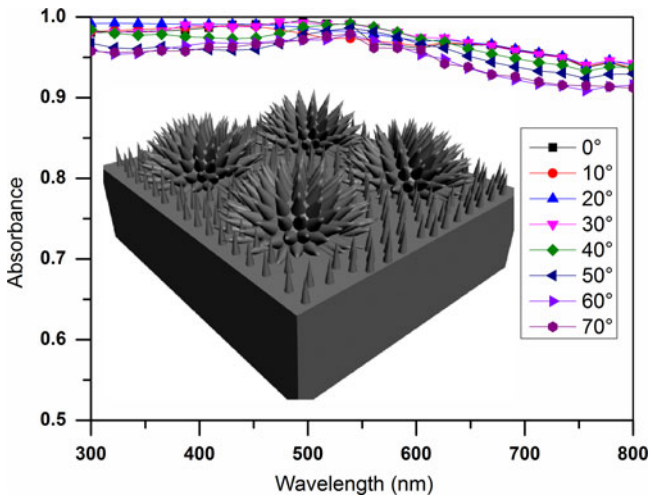


DOI: 10.1109/JPHOT.2018.2794201
1943-0655 © 2018 IEEE

IEEE photonics SOCIETY

IEEE

# Ultrabroadband Plasmonic Absorber Based on Biomimetic Compound Eye Structures

**Xiaoxuan Dong**[1, 2, 3] **and Linsen Chen**[1, 2, 3]

[1] College of Physics, Optoelectronics and Energy, Soochow University, Suzhou 215006, China
[2] Key Laboratory of Advanced Optical Manufacturing Technologies of Jiangsu Province and the Key Laboratory of Modern Optical Technologies of Education Ministry of China, Soochow University, Suzhou 215006, China
[3] College of Physics, Optoelectronics and Energy and the Collaborative Innovation Center of Suzhou Nano Science and Technology, Soochow University, Suzhou 215006, China

*DOI:10.1109/JPHOT.2018.2794201*


Manuscript received November 22, 2017; revised January 6, 2018; accepted January 9, 2018. Date of publication January 24, 2018; date of current version February 8, 2018. This work was supported by the National Natural Science Foundation of China under Grant 91323303 and by the General Programs of the National Natural Science Foundation of China under Grant 61575135. Corresponding author: Xiaoxuan Dong (e-mail: ddd5774769@163.com).

**Abstract:** A perfect absorber based on plasmonic resonance for a variety of remarkable properties has motivated vivid research during the last few decades. However, most of the perfect absorbers had been focused on polarization-insensitive and narrow-band absorption, due to the existence of a theoretical limit. It is urgent to extend the optical properties of absorbers with omnidirectional and broadband performances to satisfy the requirements for practical application. Hence, we adopt a new convenient, energy-saving, and environmentally friendly silk mediated layer nanoimprint technology to obtain biomimetic moth eye structures with omnidirectional and broadband perfect absorption. Experimental and simulation results show that the absorbers can realize the absorption efficiency to a maximum of 99% over the entire visible spectrum for angles up to 70° from normal. In addition, it also exhibits excellent bidirectional absorptive characteristic of this design. We anticipate that this absorber may have greatly potential application in the photovoltaic and thermal imaging area.

**Index Terms:** Compound eye structure, nanoimprint lithography, silk fibroin, perfect absorber.

## 1. Introduction

Perfect absorbers (PA) have attracted considerable interest due to their near unity absorbance, and polarization independence. Besides its polarization dependence, the bandwidth and angle dependence of PA also plays a crucial role in its design. To date, many concepts and structures have been researched and developed for perfect absorbers (PAs) at microwave [1], [2], terahertz [3], and infrared frequencies [4]. And the designed PAs are limited at a narrow frequency region owing to the optical property is determined by the geometry [5], [6]. However, omnidirectional and broadband PAs are desired for photovoltaic cell [7]–[9], and radar stealth [10], [11]. Recently, a few works have been presented to directly achieve a broadband perfect absorber [12], [13], whereas broadband absorber in the visible regime is still relatively scarce. This is because it is hard and complicated

to realize sub-wavelength structures in the visible regime. Quite recently, Hedayati, M. K. *et al*. [12] proposed a broadband PA consisting of a stack of metal and metal nanocomposite. Such PAs achieve broadband absorption at the visible spectrum. However, the requirement of multiple vacuum-processed steps leads to a lower throughput and higher capital cost that may limit practical device applications. Tun Cao *et al.* [13] demonstrated a metamaterial absorber composed of sandwich metal-dielectric-metal structure, which adopt prototypical Phase-change material as dielectric layer with a large imaginary part of refractive index. Such a metamaterial PA has broadband in the visible regime. However, owing to greatly heat generation in absorber lead to surface melting or reshaping [14].

In nature, moth eye nanostructure exhibits exceptional broadband and wide-angle optical performance compared with other structures [15]–[18]. Therefore, it is being commercially used for various applications such as camera lenses, light-emitting diodes, flat-panel displays, and solar cells [19]–[21]. For these reasons, numerous nanostructured fabricated methods have been emerged to achieve the moth-eye structure. Except the expensive and time-consuming methods, the colloidal lithography combining with reactive ion etching technology is a way to fabricate moth-eye structures [22], [23], which is a cheap and large-area fabrication method. However, such processes often require multiple etching steps. Mana Toma *et al*. [18] have demonstrated a single etching step to create moth-eye structure on soft substrate by combining colloidal lithography with oxygen plasma etching. However, this method is hard to extend to other substrates to limit the application regime. Another easy, low-cost and large-area fabrication method is mold replication. Po-Lin Chen *et al*. [24] exhibited a fabricating compound eye structure on glass substrate method by hot embossing technique. But this method needs special equipment to achieve. Hemant Kumar Raut *et al*. [25] showed an fabrication of multiscale ommatidial arrays method by a sacrificial layer mediated nanoimprinting technique, this structure can present almost all the characteristics of moth-eye. However, this processing procedure used poisonous solutions as mediated layer that lead to the method can't be wide expand.

Based on the above issues, we report a new and non-toxic fabrication method for the perfect plasmonic absorbers. In this approach, we employ relatively simple and environmentally friendly silk mediated layer nanoimprint technology (SML-NIL) to achieve large-area and homogeneous manufacturing biomimetic moth-eye structure. This absorber also can display all of characteristics of moth-eye that optical measurements reveal a maximum to 99% absorbance in the visible under the wide incident angle up to 70°. Fortunately, our proposed absorber also exhibit excellent dual-direction absorption property and which could be an outstanding candidate for high-efficiency absorber materials.

## 2. Fabrication of a Compound Eye Absorber

It is well known that the fabrication of three-dimensional multiscale structure is relatively cumbersome in comparison to two-dimensional nanostructure. In spite of NIL technique could also fabricate 3D structures with the assistance of laser swelling technique [26] or by means of 3D template prepared by complicated process [24], [27], these methods suffer from time-consuming, harsh technological requirement for fabricating template process, and also pose limitations in generating arbitrary multiscale structures. To overcome these challenges, we demonstrate an silk mediated layer nanoimprint technology(SML-NIL) that adopt double NIL processes to achieve compound eye multiscale structure where utilizing silk fibroin as a sacrificial layer. Silk fibroin, the natural protein extracted from the Bombyx mori caterpillar, because of its robust mechanical characteristic [28], [29], which provides the ability to prevent the any deformation of nanorods structures even at a high temperature. Meanwhile, silk fibroin is a natural non-toxic aqueous material and easy to dissolve in water for the crystallized silk during developing process, so it is very suitable as a sacrificial layer in this procedure.

The preparation process of perfect absorber is shown in Fig. 1. Firstly, nanorod arrays were fabricated by transferring the contrary mold on a polycarbonate film (PC) using nanoimprint system (Eitre3, Obducat Technologies AB, Sweden). The experiment parameters was employed by 30 bar

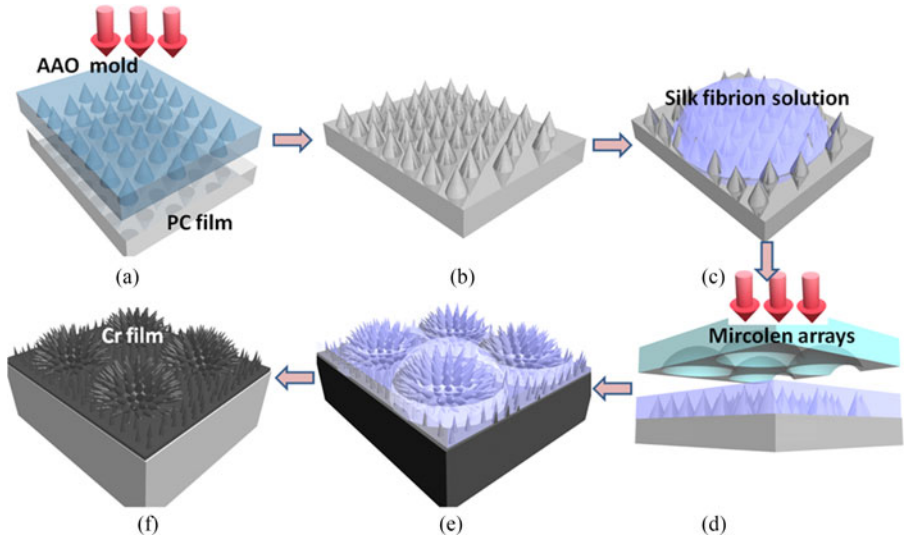


Fig. 1. The sketch of the fabricating process for the perfect absorber. (a) Utilizing AAO template to imprint nanostructures on the PC film. (b) Nanostructures on the PC film after the imprinting process, which includes quasi-periodic hexagonal distributed nanorod arrays with a height of 500 nm and a diameter of 200 nm. (c) Silk fibrion as a sacrificial layer coated on the nanostructures. (d) Mircolens array imprinted on the nanostructures surface. (e) Forming compound eye after imprinting and washing the imprinted substrate in water, thereby removing the silk film. (f) The final structures after deposition of a 30-nm chrome (Cr) layer.

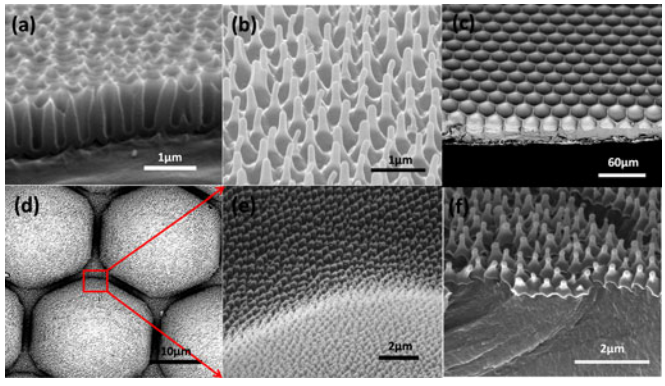


Fig. 2. The SEM images of corresponding structures in the fabricating process of a perfect absorber. (a) The SEM image of AAO mold with a diameter of 200 nm, a period of 400 nm, and a height of 500 nm. (b) Nanorod arrays on the PC film substrate after first imprinting. (c) Metallic Ni template of microlens arrays with a period of 20 $\mu$m and a depth of 8 $\mu$m. (d) Compound eye structures after second imprinting. (e) Amplifying section of compound eye structures. (f) Cross-sectional SEM image of a compound eye absorber. The upper layer is Cr film.

pressure, 150 °C temperature and 200 seconds duration time. Here, we used anodic aluminum oxide (AAO), which fabricates method referring to [24], as the contrary mold of nanorods fabricated by electrochemical etching technology. The SEM images of AAO mold and nanorod arrays are presented in Fig. 2(a) and (b), a diameter 200 nm, height 500 nm quasi-periodic hexagonal nanorod arrays was formed on the PC film substrate. Secondly, a 6% solution of silk fibroin, the fabrication method referring to [29], was spin-coated on the imprinted surface before dry-out procedure to form a thin film of $\sim$1 um silk fibrion film as seen in Fig. 1(c). And then, a second imprinting of microlens arrays with 20 um diameter, 25 um period and 8 um height was on the surface of nanorods structures coated with silk fibroin at the temperature of 150 °C to form compound eye structures

and then developed in water to remove the silk fibroin layer as displayed in Fig. 1(d) and (e). The SEM images of compound eye structures as showed in Fig. 2(c) and (d) exhibit that the nanorod arrays were fully conformal to the curved portions of the microlens and also preserved their original protuberances. The last step was deposited a thin metallic chrome (Cr) layer of 30 nm on the surface of compound eye structures by ion beam sputtering technology (LDJ-3B, Beijing Advanced Ion Beam Technology, China) as displayed in Fig. 1(f). In order to metallic layer conformal covering the surface of the compound eye, we adopted oblique deposition with angle of 5° to the sample surface and accompanied with rotating sample holder at a constant speed. The thin continuous metallic film plays the role of a perfect thermal and electric conductor in case of too much heat to gather [28].

## 3. Results and Discussion

In this design, metallic Cr was chosen as absorber material. The material is critical for realization of surface plasmonic resonance. In general, the best candidates are depended on the lower optical loss for metallic material, such as Au, Ag and Al, which are able to realize high intensity of resonance. But we find that metallic Cr is capable of achieving more absorbable from ultrathin metallic layer, even if the resonant intensity is relatively weaker than those proposed previously. Fig. 2. displays the SEM images of the corresponding structures for the perfect absorber in fabricating process.

From Fig. 2(a) and (b), we can note that there is some difference between the nanorods and the array configuration is not strictly uniform distribution. To some extent, this distribution is the reason that the optical performance of this absorber is polarization independent and reduces the diffraction efficiency on the aperiodic nanostructure arrays [30], [31]. In Fig. 2(c), it is displayed the metallic nikel (Ni) template of microlens arrays with a period of 20 $\mu$m and depth of 8 $\mu$m. From Fig. 2(d) and (e), the nanostructures array is uniformly coated on the surface of microlens even though in the intersection of microlens and horizontal plane. It is strongly suggested that silk fibrion as a sacrificial layer has excellently protected the nanostructures after hot imprinting process. In Fig. 2(f), it is obviously displayed that a 30 nm Cr film is conformal covering on the surface of compound eye nanostructures. Owing to hard to neatly cutting the edge of the sample for PC film, the surface of the sample emerges that some rending in continuous metallic layer, but it will not appear this kind of phenomenon in the actual production.

To examine the optical properties of the designed absorber, we perform a UV-VIS-NIR spectrophotometer (UV-3600, SHIMADZU) to measure the reflection and transmission. According to the equation $A = 1 - T - R$ (A = absorbance; T = transmittance; R = reflectance), we can get the absorption properties for perfect absorber. Fig. 3(a) exhibits that the absorbance curves with wavelength for different incidence angles. It is obviously displayed that a broadband absorption over the entire visible spectrum range from 300 nm to 800 nm were obtained for different incidence angles, and the inserted picture of absorber showing almost black reflection from the compound eye absorber surface also have proof that it is capable of realizing broadband absorption. This is ascribed to the morphology characteristic of sub-wavelength nanostructures, which can confine the electromagnetic field in the space between nanorods. We will illuminate the theoretical analysis in the later simulation section. The maximum absorbance attached to 99% in the compound eye absorber was exhibited by the absorptive curve. The results showed that our absorber outperforms the traditional flat moth eye absorber significantly (seen in supporting information). Moreover, omnidirectional properties had been emerged for the compound eye absorber in the plots. With the incident angle increasing, the absorber remains keep a high absorption in comparison with the flat absorber [32]. As an added bonus, we found that the light from the rear surface incident also had presented excellent absorption at the different angles, as displayed in Fig. 3(b). It is indicated that the overall absorption performance is inferior to that from the upper incidence light partly reason is mirror reflection exist at the lower interface of PC film. This will be discussed that what is resulting in this difference in the following.

The designed structures were analyzed under the framework of full-field electromagnetic simulations based on numerical solution of time-dependent Maxwell equations using the finite-difference

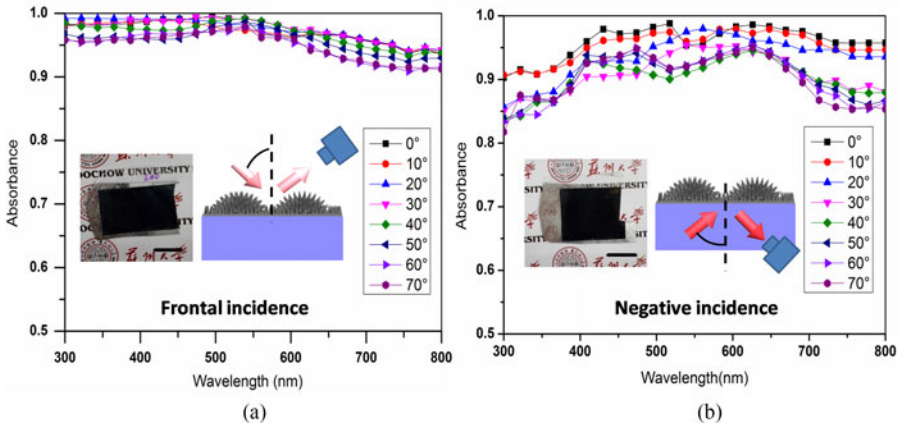


Fig. 3. Absorption spectra of a compound eye absorber with different angles of incidence. (a) For the incident light from the top down direction. (b) For the incident light from the bottom up direction. The inserted pictures and schematics show the sample of compound eye absorbers and the optical setup utilized for absorbance measurement, respectively. The scale bar is 1 cm in inserted pictures.

time-domain (FDTD) method, which is available from Lumerical software package. In order to understand the mechanism of absorption, the Poynting vector and electric field intensity distribution (Fig. 4) were calculated under positive and negative normal incident plane wave with TE polarization (x-polarization electric field) for three different wavelengths (370 nm, 550 nm and 700 nm) acting on the same geometrical parameters, respectively. The geometrical parameters of compound eye absorber here resemble that in Fig. 2(b). When incoming light with 370 nm wavelength illuminated from the positive normal direction, the field is mainly collected at each near to peak point of the nanostructures and induced the plasmonic resonance between them, which results in the perfect absorption at this frequency. Meanwhile, the poynting vector represented by red arrows along –z-direction propagates to the surface of Cr layer and most of them are absorbed by the metallic layer, while few of them through the metallic layer and propagate out the compound eye absorber. Similarly, for 550 nm and 700 nm wavelengths incident light, they also produce the same resonance in the nanostructures. Nonetheless, the position of resonance is different with that of the 370 nm. The field gradually collects trend to the middle and bottom of nanostructures, respectively. This absorption model is similar to continuous U-shaped resonators arrays arranged [33]. Due to the poynting vector rending to form vortices near the resonance point, the energy of the incident light is trapped between the nanostructures, and is finally absorbed. In the basis of the gap between adjacent nanostructures gradually changing in the z-direction, it leads to broadband absorption over the entire visible range.

However, when the incident light from the negative direction illuminating, there is also appearing the excellent absorption characteristic in this designed structure (Fig. 4(b)). Nevertheless, the principle of this absorption is disagreement to the explanation above mentioned. As displayed in Fig. 4(b), the electric field intensity distribution is mainly concentrating on the bottom of compound eye absorber. Meanwhile, the poynting vectors propagate to the internal structure with the intensity of poynting vector gradually reducing. As the wavelength increasing, the electric field intensity permeating in the internal structure becomes gradually strengthen. In spite of a few of power leaking out the absorber, this absorber performs outstanding absorption. Actually, due to the geometry of the nanostructure of absorber is similar to small concave pit for incident light, and the sidewall of nanostructure is gradually gradient variation from the bottom to top of nanostructure, the electric field intensity is unable to get gather at the top of nanostructure. The characteristic of this absorber is a resemblance to a large high-aspect ratio grating, referring to [34], where the electric field is mostly localized at the bottom of nanostructures resulting perfect absorption. Owing to the strongest plasmonic resonance induced by the bottom of the designed absorber for short wavelength, the E-field intensity is mainly distributed to the bottom of nanostructure. Meanwhile, the long wavelength

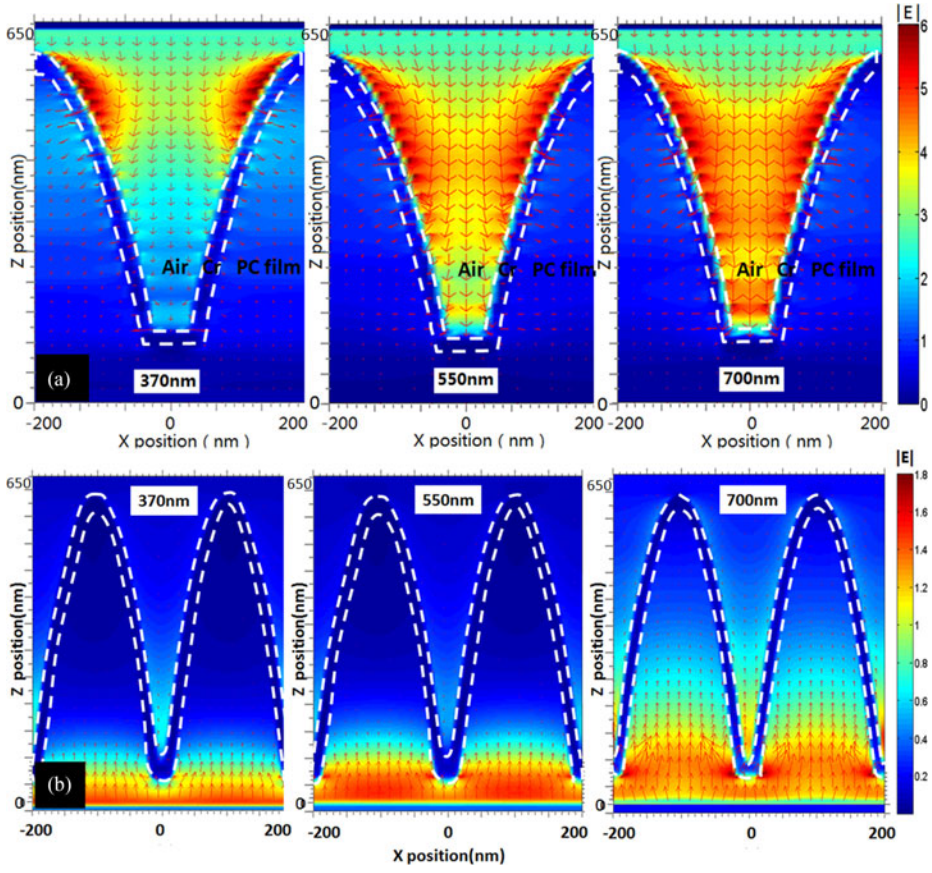


Fig. 4. Simulation results of electric field intensity and poynting vector for the incident wavelength of 370, 550, and 700 nm at the positive and negative normal directions, respectively. The red arrows and the white dashed line represent the direction of the poynting vector and the outline of the Cr layer.

is only able to induce lower plasmonic resonance leading to a portion of energy pass into the nanostructure.

## 4. Conclusion

In conclusion, we have presented an omnidirectional and broadband perfect absorber fabricating by SML-NIL technology. The introducing silk fibrion sacrificial layer covering on the surface of nanostructures exhibits excellent property of protecting nanostructures during imprinting into microlens structure. Furthermore, based on these outstanding properties, our designed compound eye absorber is well suited for solar absorbing applications involving large-scale fabricated, ultra-thin flexible substrate, further, extending applications into flexible absorbers/emitters, photoelectrolysis, and hot-electron generation. In addition, using silk fibrion as sacrificial layer method incorporated with the double imprinting technique is a potential pathway for fabrication of various 2.5 dimensions multiscale patterns with immensely diverse applications.

## References

[1] N. I. Landy, S. Sajuyigbe, J. J. Mock, D. R. Smith, and W. J. Padilla, "Perfect metamaterial absorber," *Phys. Rev. Lett.*, vol. 100, 2008, Art. no. 207402.

[2] Y. Z. Cheng, Y. Wang, Y. Nie, R. Z. Gong, X. Xiong, and X. Wang, "Design, fabrication and measurement of a broadband polarization-insensitive metamaterial absorber based on lumped elements," *J. Appl. Phys.*, vol. 111, 2012, Art. no. 044902.
[3] Y. J. Yoo *et al.*, "Polarization-independent dual-band perfect absorber utilizing multiple magnetic resonances," *Opt. Exp.*, vol. 21, no. 26, pp. 32484–32490, 2013.
[4] N. Liu, M. Mesch, T. Weiss, M. Hentschel, and H. Giessen, "Infrared perfect absorber and its application as plasmonic sensor," *Nano Lett.*, vol. 10, no. 7, pp. 2342–2348, 2010.
[5] Y. Guo, L. Yan, W. Pan, B. Luo, and X. Luo, "Ultra-broadband terahertz absorbers based on 4 $\times$ 4 cascaded metal-dielectric pairs," *Plasmonics*, vol. 9, pp. 951–957, 2014.
[6] Q. Feng, M. Pu, C. Hu, and X. Luo, "Engineering the dispersion of metamaterial surface for broadband infrared absorption" *Opt. Lett.*, vol. 37, 2012, Art. no. 2133.
[7] Y. Avitzour, Y. A. Urzhumov, and G. Shvets, "Wide-angle infrared absorber based on a negative-index plasmonic metamaterial," *Phys. Rev. B*, vol. 79, 2009, Art. no. 045131.
[8] J. Tang, Z. Xiao, and K. Xu, "Ultra-thin metamaterial absorber with extremely bandwidth for solar cell and sensing applications in visible region," *Opt. Mater.*, vol. 60, pp. 142–147, 2016.
[9] Y. Wang, T. Sun, T. Paudel, Y. Zhang, Z. Ren, and K. Kempa, "Metamaterial-plasmonic absorber structure for high efficiency amorphous silicon solar cells," *Nano. Lett.*, vol. 12, pp. 440–445, 2012.
[10] K. Iwaszczuk, A. C. Strikwerda, K. Fan, X. Zhang, R. D. Averitt, and P. U. Jepsen, "Flexible metamaterial absorbers for stealth applications at terahertz frequencies," *Opt. Exp.*, vol. 20, no. 1, pp. 635–643, 2012.
[11] X. Shen *et al.*, "Triple-band terahertz metamaterial absorber: Design, experiment, and physical interpretation," *Appl. Phys. Lett.*, vol. 101, 2012, Art. no. 154102.
[12] M. K. Hedayati, F. Faupel, and M. Elbahri, "Tunable broadband plasmonic perfect absorber at visible frequency," *Appl. Phys. A*, vol. 109, no. 4, pp. 769–773, 2012.
[13] R. E. Simpson, L. Zhang, T. Cao, C. W. Wei, and M. J. Cryan, "Broadband polarization-independent perfect absorber using a phase-change metamaterial at visible frequencies," *Sci. Rep.*, vol. 4, 2014, Art. no. 3955.
[14] X. Chen, Y. Chen, M. Yan, and M. Qiu, "Nanosecond photothermal effects in plasmonic nanostructures," *ACS Nano*, vol. 6, no. 3, pp. 2550–2557, 2012.
[15] Y. H. Ghymn, K. Jung, M. Shin, and H. Ko, "A luminescent down-shifting and moth-eyed anti-reflective film for highly efficient photovoltaic devices," *Nanoscale*, vol. 7, no. 44, pp. 18642–18650, 2015.
[16] E. Stratakis, A. Ranella, and C. Fotakis, "Biomimetic micro/nanostructured functional surfaces for microfluidic and tissue engineering applications," *Biomicrofluidics*, vol. 5, 2011, Art. no. 013411.
[17] D.-H. Ko *et al.*, "Biomimetic microlens array with antireflective moth-eye surface," *Soft Matter*, vol. 7, no. 14, pp. 6404–6407, 2011.
[18] M. Toma, G. Loget, and R. M. Corn, "Fabrication of broadband antireflective plasmonic gold nanocone arrays on flexible polymer films," *Nano Lett.*, vol. 13, no. 12, pp. 6164–6169, 2013.
[19] L. Zhou *et al.*, "Multiscale micro–nano nested structures: Engineered surface morphology for efficient light escaping in organic light-emitting diodes," *ACS Appl. Mater. Interfaces*, vol. 7, no. 48, pp. 26989–26998, 2015.
[20] T.-H. Chou *et al.*, "Fabrication of antireflection structures on TCO film for reflective liquid crystal display," *Microelectron. Eng.*, vol. 86, no. 4, pp. 628–631, 2009.
[21] V. Yerokhov, I. Melnyk, A. Tsisaruk, and I. Semochko, "Porous silicon in solar cell structures," *Optoelectron. Rev.*, no. 4, pp. 414–417, 2000.
[22] Z. Xu, Y. Chen, M. R. Gartia, and J. Jiang, "Surface plasmon enhanced broadband spectrophotometry on black silver substrates," *Appl. Phys. Lett.*, vol. 98, 2011, Art. no. 241904.
[23] A. Horrer *et al.*, "Parallel fabrication of plasmonic nanocone sensing arrays," *Small*, vol. 9, no. 23, pp. 3987–3992, 2013.
[24] P.-L. Chen, R.-H. Hong, and S.-Y. Yang, "Hot-rolled embossing of microlens arrays with antireflective nanostructures on optical glass," *J. Micromech. Microeng.*, vol. 25, 2015, Art. no. 095001.
[25] H. Ku. Raut *et al.*, "Multiscale ommatidial arrays with broadband and omnidirectional antireflection and antifogging properties by sacrificial layer mediated nanoimprinting," *ACS Nano*, vol. 9, no. 2, pp. 1305–1314, 2015.
[26] J. Shao *et al.*, "Generation of fully-covering hierarchical micro-/nano- structures by nanoimprinting and modified laser swelling," *Small*, vol. 10, no. 13, pp. 2595–2601, 2014.
[27] M. S. M. S. B. Radha, S. H. Lim, and G. U. Kulkarni, "Metal hierarchical patterning by direct nanoimprint lithography," *Sci. Rep.*, vol. 3, 2013, Art. no. 1078.
[28] H. Kwon and S. Kim, "Chemically tunable, Biocompatible, and cost-effective Metal-insulator-metal resonators using silk protein and ultrathin silver films," *ACS Photon.*, vol. 2, no. 12, pp. 1675–1680, 2015.
[29] N. E. Kurland, T. Dey, S. C. Kundu, and V. K. Yadavalli, "Precise patterning of silk microstructures using photolithography," *Adv. Mater.*, vol. 25, no. 43, pp. 6207–6212, 2013.
[30] M. G. Nielsen, A. Pors, O. Albrektsen, and S. I. Bozhevolnyi, "Efficient absorption of visible radiation by gap plasmon resonators," *Opt. Exp.*, vol. 20, no. 12, pp. 13311–13319, 2012.
[31] J. Zhang, S. Shen, X. X. Dong, and L. S. Chen, "Low-cost fabrication of large area sub-wavelength anti-reflective structures on polymer film using a soft PUA mold," *Opt. Exp.*, vol. 22, no. 1, pp. 1842–1851, 2014.
[32] F. P. G. de Arquer, A. Mihi, and G. Konstantatos, "Large-area plasmonic-crystal hot-electron-based photodetectors," *ACS Photon.*, vol. 2, no. 7, pp. 950–957, 2015.
[33] X. Xiong, S.-C. Jiang, Y.-H. Hu, R.-W. Peng, and M. Wang, "Structured metal film as a perfect absorber," *Adv. Mater.*, vol. 25, no. 29, pp. 3993–3993, 2013.
[34] T. López-Rios, D. Mendoza, F. J. G. Vidal, J. Sánchez-Dehesa, and B. Pannetier, "Surface shape resonances in lamellar metallic gratings," *Phys. Rev. Lett.*, vol. 81, pp. 665–668, 1998.